

## Epitaxial Crystal Growth of Charged Colloids

J. P. Hoogenboom,<sup>1,2</sup> A. Yethiraj,<sup>1,2</sup> A. K. van Langen-Suurling,<sup>3</sup> J. Romijn,<sup>3</sup> and A. van Blaaderen<sup>1,2</sup>

<sup>1</sup>*FOM Institute for Atomic and Molecular Physics, Kruislaan 407, 1098 SJ Amsterdam, The Netherlands*

<sup>2</sup>*Soft Condensed Matter, Debye Institute, Utrecht University, Princetonplein 5, 3584 CC Utrecht, The Netherlands*

<sup>3</sup>*Delft Institute of Microelectronics and Submicron Technology, 2600 GB Delft, The Netherlands*

(Received 24 April 2002; published 4 December 2002)

A pattern of repulsive, charged lines is shown to direct three-dimensional (3D) crystallization in a system of long-range repulsive, density-matched colloids. At volume fractions where the bulk phase behavior leads to bcc crystallization, the 1D template was found to induce formation of a metastable fcc crystal. The bcc crystals were oriented with the (100) or the (110) plane, with twofold twinning, parallel to the template. The template further induced prefreezing of the (100) plane. At a large mismatch between template and interparticle spacing, 1D strings form in the surface layer of a 3D crystal.

DOI: 10.1103/PhysRevLett.89.256104

PACS numbers: 68.35.Rh, 05.65.+b, 68.08.De, 82.70.Dd

Research on model colloids has gained renewed interest both due to their use in materials like photonic crystals, and because of their use as a condensed-matter model system with the possibility of three-dimensional real-space analysis [1,2]. Colloidal epitaxy, the manipulation of colloidal crystallization by using patterned surfaces [2], is one example of a recently introduced technique that stimulated research in both applied [3,4] and fundamental physics [5,6]. So far, experiments reported were performed on systems with short-ranged interactions and in a gravitational field [2,4,5].

In this Letter we will show the extension of colloidal epitaxy to systems with a long-ranged repulsive (LRR) interaction potential. The phase diagram of colloids with LRR interactions shows a martensitic solid-solid transition [7]. At relatively low volume fractions a transition from the liquid state to a body-centered cubic (bcc) crystal occurs, followed at higher volume fractions by a bcc to face-centered cubic (fcc) transition. The tunability of lattice parameters in these colloidal crystals by factors like ionic strength and surface potential make LRR colloids suitable for applications, like sensors and photonic switches [8].

A one-dimensional (1D) pattern of lines that has a surface charge similar to that of the colloids was used as a template. The reason for choosing a 1D substrate pattern is twofold. First, a 1D template is easy to make. Second, if perfect epitaxial growth of a 3D crystal is possible with a 1D template, we would expect a system with LR potentials to be most successful. In this respect we want to note that 3D crystal growth, and even inducing long-range 2D order, was unsuccessful with a 1D line pattern in the case of short-range attractive colloids [5]. Below it will be shown that, e.g., for a templated, square-symmetric surface plane there is no anisotropy corresponding to the 1D lines present in the 2D crystal plane anymore. The results presented here can easily be extended to more complex surface patterns by directly patterning a substrate with a surface-layer of colloids [9].

All experiments were carried out at volume fractions where bcc crystals were found to be the stable crystal phase on the time scales of our experiments (typically several days), and we therefore call this the equilibrium phase. As fcc crystal formation may proceed via formation of a bcc critical nucleus [10], we, however, cannot exclude the possibility that this bcc phase is metastable. The role of gravity in the epitaxial growth process was eliminated by nearly density-matching colloids and solvent, as well as by directing the resulting small effective gravitational force (on the order of  $-10^{-2}g$ , with  $g$  the earth gravitational constant) away from the templated wall.

In the following, the phase behavior with respect to volume-fraction and template spacing will be classified by the symmetry of colloids in the surface plane, for which we found three distinct effects. Our first observation is the formation of a square-symmetric surface plane that, depending on template spacing, was found to belong to a metastable fcc crystal as well as a bcc crystal phase. Second, we observed alignment of the bcc(110) plane along the template lines with twinning occurring deeper in the crystal. Finally, the template was found to induce purely 1D order directed along the lines. In this last case a rearrangement to a 3D ordered crystalline phase was found to take place in the first few layers. At higher volume fractions, this reconstructed crystal was still directed by the template and maintained a distorted noncubic structure extending over 30 layers deep. The global surface-induced "phase behavior" is indicated in Fig. 1. The three different effects will be discussed in detail below.

Patterns of 1000 lines, 0.550  $\mu\text{m}$  wide and 2 cm long with constant spacing, were made with electron-beam lithography in a 450-nm-thick fluorescently labeled poly(methylmethacrylate) (PMMA) layer [2]. A template and the various line spacings are shown in Fig. 1. For all images shown later the orientation of the template is the same as in Fig. 1. The colloids were fluorescently labeled,

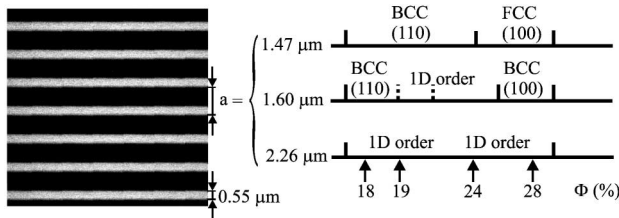


FIG. 1. Confocal image of the striped template pattern (to the left) with the width and spacings of the lines indicated. Light areas correspond to PMMA, dark areas to 450 nm lower indium-tin-oxide-coated glass. For every line spacing the phase diagram of surface-layer symmetry is given. For (110) and (100) planes the 3D crystal structure is given as well. Phase boundaries have been indicated with an accuracy of  $\pm 0.02$ , and dashed lines indicate a coexistence region between neighboring phases. Volume fractions at which a detailed 3D structure analysis was performed are indicated at the bottom.

sterically stabilized PMMA spheres [11]. In the refractive-index-matching solvent mixture used, a 0.74/0.26 volume ratio mixture of cycloheptylbromide and cis-decalin which density matches the spheres to effective gravitational force of  $-10^{-2}g$ , the sphere diameter is 1.05  $\mu\text{m}$  (polydispersity less than 0.05). The surface potential was found to be 100 mV with  $\kappa r \leq 2.5$ , with  $\kappa$  the inverse Debye length and  $r$  the radius of the spheres [12].

A 100- $\mu\text{m}$ -thick capillary sample cell was made with the template mounted on the bottom side corresponding to the highest effective gravitational energy. Samples were analyzed using fluorescence confocal microscopy (Leica TCS-SP2, 100 $\times$  NA). A gradient in particle volume fraction along the template lines was created, which was, after equilibration,  $(4 \pm 1)$  vol % over 2 mm lateral size. The 3D particle coordinates were retrieved as described in Ref. [2]. For the volume fractions indicated in Fig. 1, a detailed analysis was performed starting with calculation of the linear number density as a function of

distance to the template,  $\rho_z$ , by integration of 3D particle coordinates over the coordinates parallel to the template. For all volume fractions  $\rho_z$  showed layering due to the presence of the wall and to crystallization. Layers were defined through the clear minima in  $\rho_z$ . Particles in the same layer were used to calculate 2D-order parameters, such as the 2D coordinate autocorrelation function (2D-CACF) and its radial average the 2D radial distribution function [2D- $g(r)$ ]. The volume fraction at a specific point in our sample was measured by direct particle counting and checked by measuring the dimensions of the crystal lattice of untemplated bcc crystals. At the low volume-fraction end ( $\varphi \approx 0.10$ ) the structure was liquidlike, while at the higher volume-fraction end ( $\varphi \approx 0.30$ ), at an untemplated wall, the sample contained bcc crystals only.

*Square symmetry [fcc/bcc(100)].*—A square-symmetric arrangement of spheres at the template, as shown in Fig. 2(a), was found at volume fractions between 0.24–0.28 and template spacings of 1.47 and 1.60  $\mu\text{m}$ . We attribute the local out-of-plane displacements, like in the lower left corner of Fig. 2(a), to stress relaxation due to a small template-crystal mismatch [13]. In the linear number density  $\rho_z$  [Fig. 2(b)], this effect can be seen as a decrease in peak height and an increase in peak width from layers one to four. The structure, however, remains clearly layered and the interlayer spacing was found to have a constant value of  $\Delta z = 1.12 \pm 0.01$   $\mu\text{m}$ .

For layers one and four the 2D- $g(r)$  is given in Fig. 2(c). As can be seen all peak positions are in perfect correspondence with an ideal lattice for both layers. The positions of neighboring particles remain unaltered despite the broadening of layers in  $\rho_z$ . The in-plane nearest-neighbor distance is  $d = (1.44 \pm 0.02)$   $\mu\text{m}$ , which indeed has a small mismatch with the template spacing of 1.47  $\mu\text{m}$ . The ratio  $d/\Delta z = 1.29$  shows that the 3D

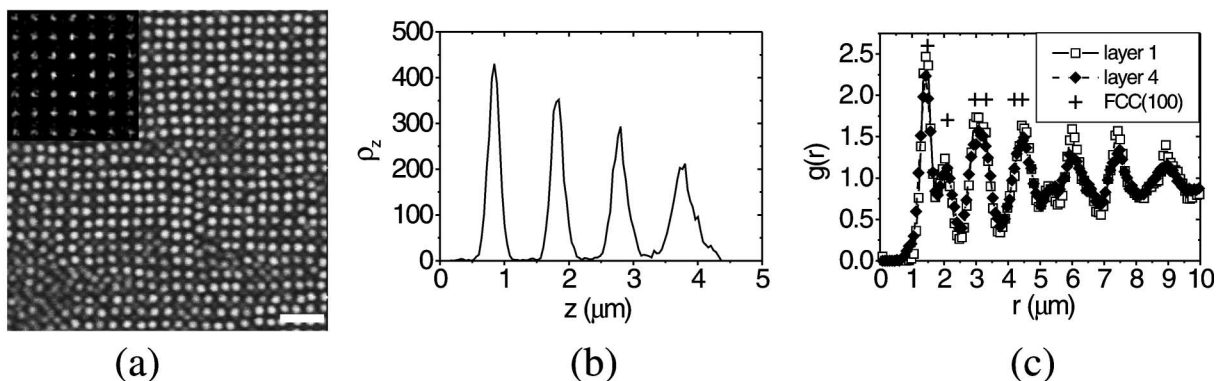


FIG. 2. (a) Confocal image of the fifth layer in a templated, (100) oriented fcc crystal ( $\varphi = 0.28$  and  $a = 1.47$   $\mu\text{m}$ ). The inset shows the 2D coordinate autocorrelation graph of the corresponding surface layer, calculated using the full 3D particle coordinates. (b) The 2D density in the direction perpendicular to the template. (c) Radial distribution functions for layer one (open squares) and layer four (filled diamonds). Open circles indicate the positions of the first six different neighbor distances in an ideal fcc or bcc (100) plane. Scale bar indicates 5  $\mu\text{m}$ .

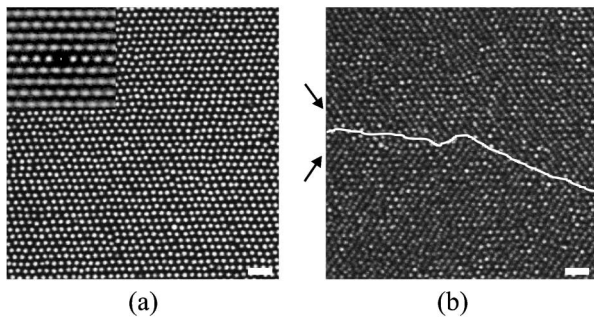


FIG. 3. Confocal images focused (a) at a surface layer with bcc(110) symmetry, and (b) between the second and third layers above (a) ( $a = 1.60 \mu\text{m}$ ,  $\phi = 0.18$ ). The inset of (a) shows the corresponding 2D coordinate autocorrelation graph. The arrows in (b) denote the two twinned orientations visible in the two-layer bcc(110) projection. The white line indicates the grain boundary. Scale bar length is  $5 \mu\text{m}$ .

structure is a metastable fcc crystal ( $d/\Delta z \sim \sqrt{2}$ ). At similar volume fractions but a larger line spacing of  $1.60 \mu\text{m}$ , we observed  $d/\Delta z$  values of 1.88, corresponding to a bcc crystal structure ( $d/\Delta z \sim 2$ ), as indicated in Fig. 1.

The average width of the 2D-CACF peaks [see inset of Fig. 2(a)] in the directions parallel and perpendicular to the template lines was found to be equal within the error margins. Thus combined LR line-sphere interactions for the (100) plane induce 2D crystalline order that bears no anisotropy of the 1D template anymore.

Finally, we want to note that this template was found to induce preezing of one to two square-symmetric layers at volume fractions where both the bulk structure as well as the surface layers at a plain wall were liquidlike. This is in qualitative agreement with recent findings of Heni and Löwen who showed that for a hard-sphere system 2D surface patterns can induce strong preezing before

bulk crystallization or preezing at a smooth wall occurs [6].

*The bcc(110).*—At a plain, untemplated wall bcc crystals orient with the densest plane, the (110) plane, parallel to the wall. Figure 3(a) shows how the line template orients the bcc(110) plane. Two of the four nearest neighbors, at a distance  $d$ , are aligned along the direction of the template lines. The other two nearest neighbors can orient at an angle of  $\pm 54.74^\circ$  with the template lines, but the line template frustrates the position of the two next-nearest neighbors at  $1.15d$  [see Fig. 3(a)]. The 3D orientation of a bcc single crystal is given by the striped pattern that is visible when successive bcc(110) layers are being projected [Fig. 3(b)]. As can be seen, twofold twinning shows up immediately above the surface layer. The angle between the two orientations was measured to be  $110(\pm 1)^\circ$ , in correspondence with the values given before.

The 2D-CACF shows that positional correlations along the template lines are weaker than those perpendicular to the lines. The average full width at half maximum of correlation peaks up to second order is 1.5 times larger in the direction parallel to the lines than perpendicular to the lines. Contrary to the (100) plane, the 1D pattern of lines in this case does not fit with the (110) symmetry, which results in a potential of mean force between spheres in which the 1D template potential can still be recognized.

*The 1D ordering.*—At a line spacing of  $2.26 \mu\text{m}$ , particles in the surface layer have a 1D symmetry, with no positional correlation between particles in successive rows [Fig. 4(a)]. The increase in the template spacing lowers the potential minimum between the lines, eventually screening sphere-sphere interactions from neighboring rows. Apparently, also combined interactions of spheres in successive rows via spheres in the second layer are too small compared to the interactions between

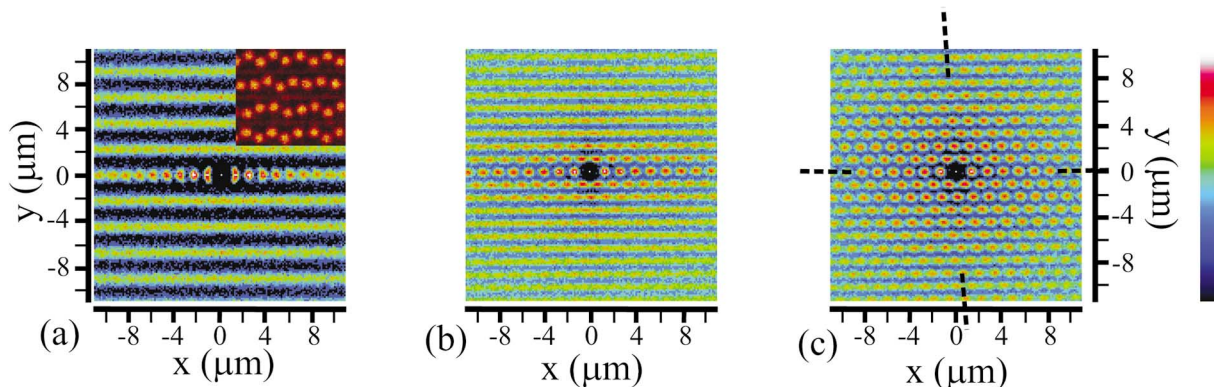


FIG. 4 (color). The 2D coordinate autocorrelation graphs for a system exhibiting a 1D ordered surface plane ( $a = 2.26 \mu\text{m}$ ,  $\phi = 0.24$ ) at (a) the surface layer, (b) layers four and five with coordinates from both layers projected onto a single plane [which causes the frequency doubling compared to (a)], and (c) a depth of  $15 \mu\text{m}$  using again a two-layer projection. The color table is given on the right (blue = 0, white = 1). The inset of (a) shows a confocal image of the surface layer to demonstrate the buckling of particles. The dashed lines in (c) indicate the two in-plane lattice directions.

spheres and lines to induce 2D in-plane ordering, even in the higher volume-fraction end of the bcc regime shown here. At low volume fractions ( $\varphi = 0.18, 0.19$ ) the structure reconstructs in a few layers to polycrystalline bcc. With increasing volume fraction, however, the line-pattern templates particle positions in the second layer as well. Here the relative contribution of the lines to the potential, both directly and through the 1D string liquid in the first layer, compared to the contribution of neighboring spheres, is smaller, which gives rise to the emergence of 2D, and thus 3D order [Figs. 4(a)–4(c)]. At a volume fraction of 0.24, the oriented crystal extends at least 60  $\mu\text{m}$  (over 100 layers), which was our maximum depth of view. Note the perfect correspondence for the positions of rows of particles in Figs. 4(a)–4(c), which is exactly the template spacing of 2.26  $\mu\text{m}$ .

In the surface layer positional correlations between next-nearest neighbors in the direction of the template lines are more localized than correlations between nearest neighbors due to a buckling of particles within the lines [Fig. 4(a)]. The addition of isotropic nearest-neighbor interactions to a single line-sphere-line interaction potential gives rise to a shift of the single, parabolic minimum to two minima, slightly displaced from the centerline. Here the increase in sphere-line energy will be overcome by a decreased sphere-sphere potential. Comparing Figs. 4(a)–4(c), it can be seen that this buckling is not present anymore as 3D ordering emerges.

The ratio between nearest-neighbor distances parallel and perpendicular to the template direction in Fig. 4(c) (i.e., along the dashed lines) is 1.61. Planes with similar symmetry can be found in fcc and hexagonal close packed (hcp) crystals, but with ratios of  $\sqrt{2}$  and  $\sqrt{3}$ , respectively. The distance between successive planes has a constant value of  $d/2.07$ . We expect this stressed body-centered tetragonal crystal to relax to either bcc or fcc in the bulk, but it was found to extend at least 30 layers deep. Indicative of a relaxation process, the angle between the two in-plane lattice directions in Fig. 4(c) is slightly off from  $90^\circ$ , namely,  $86(\pm 1)^\circ$ . Further experiments have indicated that the ratio between the lengths of the in-plane lattice vectors in at least the first 12 layers can be stretched to values approaching 1.7 by changing the line-width. In this way it may be possible to grow an hcp crystal of spheres with a LRR interaction. At the smaller line distance of 1.60 (see Fig. 1), we did observe planes where this in-plane ratio was 1.37, almost equal to the ideal fcc(110) ratio, but here the interlayer distance was not constant in the first four layers and the structure reconstructed to tilted bcc(110) hereafter. These results indicate that more complex colloidal surface and bulk phases can be induced in systems with LRR interactions when more elaborate surface patterns, for instance, by directly patterning colloids on a surface [9], are created. By dissolving a polymerizable precursor, these structures

can be solidified in a polymer matrix for device applications [8].

In conclusion, we have shown the possibility of epitaxial growth of colloids with long-ranged repulsive interactions in a density-matched system, where epitaxial growth is solely driven by the substrate potential. This substrate potential was created by 1D charged lines, which were found to direct 3D crystal structure over a broad range of volume fractions. Among our observations is the growth of a metastable fcc crystal. At increasing line spacing, the structure in the surface layer changes to a 1D string liquid due to screening of sphere-sphere interactions by the line potential. At increasing volume fractions, the substrate potential of the template induces ordering in layers beyond the surface layer, until at a volume fraction of 0.24 a 3D crystalline structure is observed that maintains a metastable noncubic structure for over 30 layers deep. At volume fractions where structure is liquidlike, the 1D template was found to induce prefreezing of one to two square-symmetric layers.

We thank S. Auer and D. Frenkel for helpful and stimulating discussions and a critical reading of this manuscript. This work is part of the research program of the “Stichting voor Fundamenteel Onderzoek der Materie (FOM),” which is financially supported by the “Nederlandse organisatie voor Wetenschappelijk Onderzoek (NWO).”

- 
- [1] A. van Blaaderen and P. Wiltzius, *Science* **270**, 1177 (1995); A. D. Dinsmore *et al.*, *Appl. Opt.* **40**, 4152 (2001).
  - [2] A. van Blaaderen, R. Ruel, and P. Wiltzius, *Nature (London)* **385**, 321 (1997).
  - [3] Y. Lu, Y. D. Yin, and Y. N. Xia, *Adv. Mater.* **13**, 34 (2001); O. Pouliquen, M. Nicolas, and P. D. Weidman, *Phys. Rev. Lett.* **79**, 3640 (1997).
  - [4] P. V. Braun *et al.*, *Adv. Mater.* **13**, 721 (2001).
  - [5] K.-H. Lin *et al.*, *Phys. Rev. Lett.* **85**, 1770 (2000).
  - [6] M. Heni and H. Löwen, *J. Phys. Condens. Matter* **13**, 4675 (2001); *Phys. Rev. Lett.* **85**, 3668 (2000).
  - [7] E. B. Sirota *et al.*, *Phys. Rev. Lett.* **62**, 1524 (1989); F. El Azhar *et al.*, *J. Chem. Phys.* **112**, 5121 (2000).
  - [8] J. H. Holtz and S. A. Asher, *Nature (London)* **389**, 829 (1997); G. S. Pan, R. Kesavamoorthy, and S. A. Asher, *Phys. Rev. Lett.* **78**, 3860 (1997).
  - [9] J. P. Hoogenboom *et al.*, *Appl. Phys. Lett.* **80**, 4828 (2002).
  - [10] P. R. ten Wolde, M. J. Ruiz-Montero, and D. Frenkel, *Phys. Rev. Lett.* **75**, 2714 (1995); S. Alexander and J. P. McTague, *Phys. Rev. Lett.* **41**, 702 (1978).
  - [11] L. Antl *et al.*, *Colloids Surf.* **17**, 67 (1986); G. Bosma *et al.*, *J. Colloid Interface Sci.* **245**, 292 (2002).
  - [12] A. Yethiraj and A. van Blaaderen, *Nature (London)* (to be published).
  - [13] J. P. Hoogenboom *et al.* (to be published).